JOURNAL OF APPLIED ELECTROCHEMISTRY **29**: 165–170, 1999.

Structure investigations of SOFC anode cermets Part II: Electrochemical and mass transport properties

J. DIVISEK, R. JUNG, I. C. VINKE

Institute of Energy Process Engineering, Research Centre Jülich, 52425 Jülich, Germany

Received 13 May 1997; accepted in revised form 22 April 1998

An approximate description of the SOFC cermet structure was performed on the basis of a combined optical and porosimetric structure analysis of the SOFC cermet anode and the results are described using the example of the SOFC substrate anode (anode with increased layer thickness). The electrode assembly consists of two layers. The electrochemically active layer of 70–90 μm corresponding the penetration depth of the electric field is located near the ZrO_2 electrolyte. This layer thickness is also a function of porosity and pore radius distribution. The remaining electrode up to a layer thickness of about 2 mm basically acts only as a current and mass distributor. The corresponding diffusion overvoltage as a function of the structural properties was calculated.

Keywords: *active layer*, *cermet anode*, *diffusion layer*, *substrate anode*

List of symbols

c	hydrogen concentration (mol cm^{-3})
c_d	hydrogen concentration outside of δ_λ (mol cm^{-3})
c_s	hydrogen concentration at the boundary cermet/bulk electrolyte (mol cm^{-3})
C_1, C_2	integration constants, Equation 11 (V)
D_{eff}	effective diffusion coefficient (cm^2 s^{-1})
D_{eff}	effective diffusion coefficient inside of λ (cm^2 s^{-1})
D_g	mean hydrogen diffusion coefficient in the gas phase (cm^2 s^{-1})
D_{kn}	Knudsen diffusion coefficient (cm^2 s^{-1})
F	Faraday constant (A s mol^{-1})
i	microkinetic current density (A cm^{-2})
i_d	macrokinetic current density (A cm^{-2})
i_m	current density in metal phase (A cm^{-2})
i_e	current density in electrolyte phase (A cm^{-2})
j_0	apparent exchange current density (A cm^{-2})
j_{00}	true internal exchange current density (A cm^{-2})
K	proportionality constant, Equation 10 (cm^{-2})
L	cermet electrode thickness
p_{H_2}	hydrogen partial pressure (bar)
$p^0_{H_2}$	reference hydrogen partial pressure (bar)
r_p	mean effective pore radius (cm)
R_i	electrochemical volume resistivity (Ω cm^3)
R_{mes}	measurable cell resistivity (Ω cm^2)
R_w	true internal electrochemical resistivity (Ω cm^2)
S_t	internal electrochemical active specific surface area (cm^{-1})
T	temperature (K)
x	axial length coordinate (cm)
$x^0_{H_2}$	molar fraction of hydrogen concentration

Greek symbols

α	reciprocal of the square root of the penetration depth of electrical field (cm^{-1})
δ	diffussion layer thickness outside the penetration depth (cm)
δ_λ	diffussion layer thickness inside the penetration depth (cm)
ε	porosity
η	overvoltage (V)
λ	penetration depth of electrical field (cm)
ρ_m	effective resistivity of the metal phase (Ω cm)
ρ_e	effective resistivity of the electrolyte phase (Ω cm)
σ_m	effective conductivity of the metal phase (Ω^{-1} cm^{-1})
σ_e	effective conductivity of the electrolyte phase (Ω^{-1} cm^{-1})
ϕ_m	potential in the metal phase (V)
ϕ_e	potential in the electrolyte phase (V)

1. Introduction

The SOFC anode consists of Ni/ZrO_2 cermet (ceramic metal), that is, of a sintered mixture of metallic (Ni) and ceramic (ZrO_2) particles. The cermet composition and preparation as well as the experiments were described in detail in the first part [1]. In the electrode assembly, the nickel phase provides electronic conduction and the ceramic electrolyte phase ionic conduction. This means that the electrode is electrochemically active within a spatially extended zone and its electrochemical properties correspond to those of a porous electrode [2, 3] and can be treated analogously.

A complete numeric model description of the SOFC cermet system, which requires a coupled

mathematical treatment of mass and charge fluxes [4], can be simplified in many cases, if it is possible to decouple the fluxes.

Finite integration technique (FIT) computer programs were developed for a reliable SOFC anode design [4, 5]. These numeric simulation programs can provide reliable results in a rigorous way, but are mathematically very sophisticated and less flexible for handling. They are appropriate, in particular, when reliable and precise input data are available, which has not been the case to date. Otherwise, approximate solutions are more useful and much simpler. In the case of an approximate solution, the mass and charge fluxes may be calculated separately by decoupling the individual fluxes, even if this is not a rigorous procedure. In this case, however, it must be ensured that the prerequisites for simplified calculations are fulfilled. This should be verified as follows using the example of an SOFC substrate anode with a thickness of up to 2 mm [6]. It can be demonstrated by the FIT computer simulation of an SOFC cermet anode [4] that the change in concentration distribution is only about 1% for the usual SOFC cell load even under unfavourable concentration conditions of the H_2 fuel gas, that is the concentration along the width coordinate is practically constant. The irregularities in H_2 concentration distribution are produced by the change from gas channel to current supply connector.

2. Assumptions of the approximate solution

The procedure for an approximate calculation may then be as follows:

(i) The internal structure of the electrodes is described assuming a porous electrode geometry.
(ii) The FIT programs show [4] a largely homogeneous distribution of the gas concentrations in the electrode structures above an electrode thickness of 500 μm. The gas distribution for these thicknesses can therefore be described as a one-dimensional problem in the x-coordinate direction. The calculations show, moreover, that the electric field has a much smaller penetration depth than the diffusion layer, which practically extends over the entire electrode thickness, so that the gas concentrations inside the electrochemically active layer may be assumed as constant.
(iii) On account of the unidimensionality, the formulations known from the theory of porous electrodes [2, 3, 7], which are of a one-dimensional nature, were used as a first approximation to calculate the electrochemical properties of the anode.

This procedure decouples the differential equations of the electric field and the concentration field, which is not necessary in numeric computer simulations. On the other hand, the solutions are much simpler and easier to handle. The issue will be treated by the example of calculating the structure data and electrochemical properties of the SOFC cermet anode with increased layer thickness (substrate anode). The first information required for calculation is the correlation between the inner structure of the SOFC cermet electrode and its electrochemical properties and the possibility of inferring the electrochemical activity from an analysis of the inner structure of this electrode. This problem was dealt with in Part I [1]. The present part of the studies serves to derive the resulting electrochemical and mass transport-induced consequences.

3. Approximate description of the SOFC anode

It can be assumed [4] that the concentration of the gases remains constant in the entire layer region. The electrochemically measured integral current density, i, is a function of the overvoltage, η, as

$$i(\eta) = \frac{1}{R_{\text{mes}}} f(\eta) \tag{1}$$

where R_{mes} is a resistivity value. In the case of planar electrodes, Equation 1 is normally written as

$$i(\eta) = 2j_{00} \sinh\left(\frac{F\eta}{2RT}\right) \tag{2}$$

where j_{00} is the exchange current density relative to the unit area. In the case of porous electrodes η is a function of the electrode thickness and Equation 2 is no longer applicable in this form. In this case, j_{00} is a part of the electrochemically active source current between the two phases (electrolyte and nickel) and the correct calculation of η as a function of the electrode depth x has the form of a differential equation requiring a very complicated solution [8]. The shape of the function $j_{00} \sinh(\eta)$ depends on the value of the prefactor j_{00} in the range of small overvoltages η. In the SOFC fuel cells, the reaction kinetics is very fast due to the high working temperature of almost 1000 °C, so that the exchange current density j_{00} has a high value. Consequently, the function according to Equation 2 is of a largely linear nature in the range of small overvoltages η, as shown in Fig. 1 according to [9]. This corresponds in Equation 1 to the function value $f(\eta) = \eta$. The one-dimensional continuum model of porous electrodes, which is schematically shown in Fig. 2, is characterized by two overlapping phases: the ion-conducting electrolyte phase (subscript 'e') and the electronically conducting metal phase (subscript 'm'). The basic equations of the model can be listed as follows [7]:

Current balance in the metal phase

$$\frac{\mathrm{d}i_{\text{m}}(x)}{\mathrm{d}x} = +S_{\text{t}} i[\eta(x)] \tag{3}$$

Current balance in the electrolyte phase

$$\frac{\mathrm{d}i_{\text{e}}(x)}{\mathrm{d}x} = -\frac{\mathrm{d}i_{\text{m}}(x)}{\mathrm{d}x} \tag{4}$$

The internal specific surface S_{t} has already been defined in [1]. The two currents, $i_{\text{m}}(x)$ and $i_{\text{e}}(x)$, are

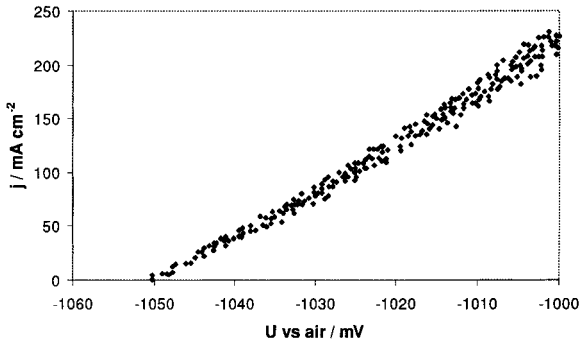

Fig. 1. Current–voltage curve of hydrogen oxidation at the SOFC cermet anode $t = 1000\,^{\circ}C$, 97% H_2, 3% H_2O, curve *IR*-corrected.

defined for the cross-sectional area in the direction of the current flow. Additional equations are

Ohm's law for the metal phase

$$\frac{d\phi_m(x)}{dx} = +\rho_m i_m(x) \tag{5}$$

Ohm's law for the electrolyte phase

$$\frac{d\phi_e(x)}{dx} = +\rho_e i_e(x) \tag{6}$$

definition of the overpotential

$$\eta(x) = \phi_m(x) - \phi_e(x) \tag{7}$$

general electrochemical kinetics

$$\begin{aligned} i[\eta(x)] &= \frac{2F}{RT} j_{00}\eta(x) \\ i[\eta(x)] &= \frac{1}{R_w}\eta(x) \end{aligned} \tag{8}$$

From Equations 3–7 the differential equation

$$\frac{d^2\eta}{dx^2} = (\rho_m + \rho_e) S_t \frac{2F}{RT} j_{00}\eta \tag{9}$$

is obtained. With $(\rho_m + \rho_e) S_t \frac{2F}{RT} j_{00} = K$, Equation 9 can be written as

$$\frac{d^2\eta}{dx^2} = K\eta \tag{10}$$

with the boundary conditions

$$\begin{aligned} &x = 0\colon\ \eta = \eta(0) \\ &\frac{1}{\rho_m}\frac{d\eta}{dx}\bigg|_{x=L} = -\int_0^L \frac{di_m}{dx}\,dx \end{aligned} \tag{10a}$$

where L is the electrode thickness. The solution of Equations 10 and 10a is given by

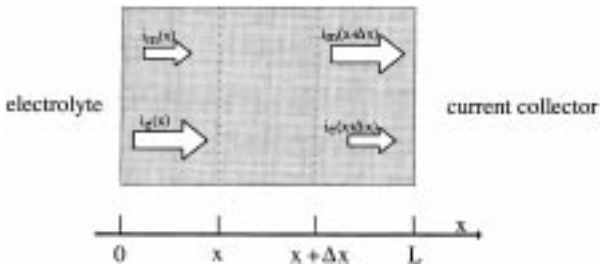

Fig. 2. Continuum model of porous electrodes.

$$\eta = C_1 e^{\alpha x} + C_2 e^{-\alpha x} \tag{11}$$

with $\alpha = \sqrt{K}$. The following is true for the constants C_1 and C_2

$$\begin{aligned} C_1 &= \eta(0)\frac{\rho_m - (2\rho_m + \rho_e)e^{-\alpha L}}{2\rho_m - (2\rho_m + \rho_e)(e^{\alpha L} + e^{-\alpha L})} \\ C_2 &= \eta(0)\frac{\rho_m - (2\rho_m + \rho_e)e^{\alpha L}}{2\rho_m - (2\rho_m + \rho_e)(e^{\alpha L} + e^{-\alpha L})} \end{aligned} \tag{11a}$$

The quantity $\alpha^{-1} = K^{-1/2}$ is defined as the penetration depth λ of the electric field into the porous electrode structure. The macrokinetic current density i_d is given by the equation

$$\begin{aligned} i_d &= -\frac{1}{\rho_e}\frac{d\eta}{dx}\bigg|_{x=0} = -\frac{1}{\rho_e}(\alpha C_1 - \alpha C_2) \\ i_d &= -\frac{\alpha\eta(0)}{\rho_e}\frac{(e^{\alpha L} - e^{-\alpha L})}{\left(\frac{2\rho_m}{2\rho_m + \rho_e} - e^{\alpha L} - e^{-\alpha L}\right)} \end{aligned} \tag{12}$$

This current density i_d can be defined by the relation

$$i_d = \frac{2F}{RT} j_0\,\eta(0) \tag{13}$$

where j_0 is the measurable macrokinetic exchange current density.

In the following, the correlation between the apparent exchange current density, j_0, and the internal active surface, S_t, will be considered for two limiting cases: on the one hand, for the case where the electrode thickness is smaller than the penetration depth of the electric field, as was studied in [1], and, on the other hand, for the so-called substrate cell [6] in which the electrode thickness can be regarded as infinitely large (also see Fig. 3).

Further computation uses the resistivities R_{mes}, R_i, R_w, which are readily available and equivalently describe the electrochemical properties, instead of the exchange current density j_0 for characterizing the electrochemical properties.

4. Evaluation of the electrochemically active layer

4.1. *Substrate electrode*

It is currently only possible to measure total cell voltages on the SOFC substrate cells [6] due to the extremely thin electrolyte layer thicknesses ($\sim$10–20 μm), also cf. Fig. 3. For experimental reasons, it is not yet possible to determine electrochemical overvoltages on the SOFC substrate anodes. Therefore, SOFC cermet anodes 100 μm in thickness produced by the WPS method (wet powder spraying) [11] were measured and evaluated, as shown in Fig. 1

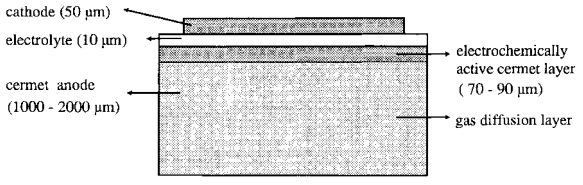

Fig. 3. Schematic diagram of an SOFC substrate cell.

of [1]. It was assumed that their basic electrochemical properties (mechanism of electrode reaction and exchange current density) are independent of the design geometry and therefore transferable to an identically produced substrate anode. In an SOFC cermet electrode, the resistivity of the electronically conducting Ni phase, ρ_m, is smaller by at least three powers of ten than that of the electrolyte phase, ρ_e. Therefore, $\rho_m + \rho_e \rightarrow \rho_e$ can be substituted in Equation 9. With the resistivity of the electrolyte layer corrected for porosity, $\rho_e\,(\Omega\,\mathrm{cm})$, and the active inner surface S_t, defined in the sense of [1], the one-dimensional differential equation of the electric field in the porous electrode (Equation 10) can then be written as

$$\frac{d^2\eta}{dx^2} = \frac{1}{\sigma_e}\frac{1}{R_i}\,\eta \tag{14}$$

with the quantities R_i (volume resistivity, $\Omega\,\mathrm{cm}^3$, and σ_e (conductivity of the electrolyte phase, $\Omega^{-1}\,\mathrm{cm}^{-1}$). With $L \rightarrow \infty$ the expression

$$\eta(x) = \eta(0)\exp\left(-\frac{x}{\lambda}\right) \tag{15}$$

is obtained for the potential profile in the SOFC cermet anode, where $\eta(0)$ is the measured overvoltage and λ the penetration depth of the electric field into the porous cermet structure. The penetration depth is calculated according to Equation 16

$$\lambda = \sqrt{\sigma_e R_i} \tag{16}$$

By the approximation $\rho_m/\rho_e \rightarrow 0$, $e^{\alpha L} \gg e^{-\alpha L}$, according to Equation 12 the macrokinetic current density i_d will be obtained as

$$i_d = \eta(0)\sqrt{\frac{\sigma_e}{R_i}} \tag{17}$$

Reduced Equation 12 in the form of Equation 17 shows that the relative error is approximately $2e^{-\alpha L}$ that is, less than 30% for $L/\lambda = 1$. To evaluate the volume resistivity R_i, its dependence on the respective H_2 partial pressure, p_{H_2}, with the corresponding temperature dependencies is required. The concentration dependence of current density on hydrogen partial pressure p_{H_2} is given by the exponent 0.25 [9]. A very small dependence (exponent ~0.1) was found for the water partial pressure. At a reference partial pressure of $p_{H_2} = 0.5$ bar, Equation 17 has the following appearance for $\eta(0)$ as the degree of polarization measurable in front of the anode and caused by the current density i_d:

$$\eta(0) = i_d\sqrt{\frac{R_i}{\sigma_e}} = i_d R_{mes}\left(\frac{0.5}{p_{H_2}}\right)^{0.25} \tag{18}$$

where R_{mes} is the measurable resistivity at $p_{H_2} = 0.5$ bar in $\Omega\,\mathrm{cm}^2$. The quantity σ_e is determined according to the formula derived from the geometry assumption [4]:

$$\sigma_e = \tfrac{2}{3}(1-\varepsilon)3.34 \times 10^2\,\exp[-10300/T] \tag{19}$$

It may be assumed for the volume resistivity R_i that it is composed of an electrochemical resistivity fraction R_w, which, analogously to the source current j_{00}, is only a function of temperature and of the ZrO_2/Ni interphase properties in the cermet, and of the internal surface S_t in the form of

$$\frac{1}{R_i} = \frac{S_t}{R_w} \tag{20}$$

To describe the electrode properties, as desired, it is necessary to know the size of the active internal surface S_t and its dependence on the effective pore radius r_p. On the basis of geometry assumptions concerning the structure of porous electrodes, it is possible to derive the approximated expression for the internal surface S_t, which adequately describes the ascent of the curves in Fig. 12 in [1], in the form of

$$S_t = \frac{1-\varepsilon}{r_p}\sqrt{\frac{4\varepsilon^2}{\pi}} \tag{21}$$

considering the published data (Table 4 in [1]) and the approximation of $S_t = S_i$ (Equation 5 in [1]). The quantity ε represents the porosity of the electrochemically active layer and r_p is the mean effective pore radius.

For evaluation purposes, an electrode must be used whose electrochemical and structural data are known. The corresponding structure analyses were described in detail and shown in tabular form in [1]. The relevant data are compiled in Table 1. The corresponding typical integral potential/current density curve is shown in Fig. 2 of [1].

The quantity R_w is the kinetically 'true' electrochemical resistivity. Its value can be calculated from Equation 20 with the aid of Equations 21 and 18 after substituting the experimentally determined values r_p and ε in Equation 21. The penetration depth λ can be calculated from Equation 16.

The layer thickness λ is a function of the porosity ε and the pore radius r_p (or the pore diameter d). The corresponding dependencies are shown in Figs 4 and 5.

The layer thickness should be kept small, that is, the electrochemical layer must have a small pore diameter and high porosity. Since, from a practical aspect, the value of $0.5\,\mu\mathrm{m}$ represents the smallest producible pore diameter and 0.5 is the highest possible porosity, the dependencies are shown for these parameters. Allowing for the fact that

$$(\rho_m + \rho_e)S_t\frac{2F}{RT}j_{00} = K = \frac{1}{\sigma_e R_i} \tag{22}$$

Table 1. Microstructure and electrochemical data of three cermet electrodes

R_w data calculated for $t = 950\,^\circ\mathrm{C}$ and $p_{H_2} = 20$ kPa

	ε	r_p /μm	S_i /cm^{-1}	R_{mes} /Ω cm^2	R_w /Ω cm^2
A	0.47	0.29	0.98×10^4	0.34	29.4
B	0.45	0.23	1.24×10^4	0.34	37.2
C	0.35	0.25	1.01×10^4	0.30	27.3

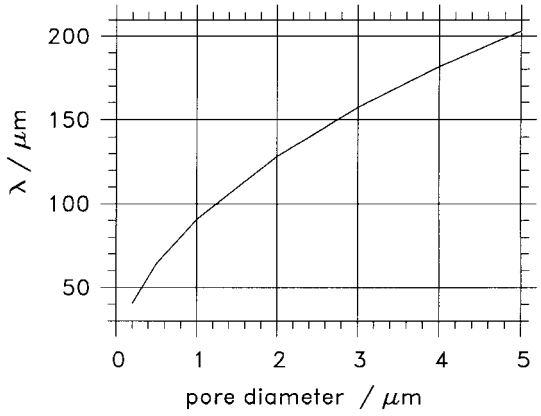

Fig. 4. Calculated dependence of the electrochemically active layer thickness λ on the pore diameter for a constant porosity of 0.5, working temperature 1223 K.

a comparison of Equations 13 and 18 shows that the dependence between the measurable current density j_0 and the internal electrochemically active surface S_t should follow the theoretical relation

$$j_0 = \sqrt{\frac{\sigma_e RT}{2F} S_t j_{00}} \tag{23}$$

that is $j_0 \approx \sqrt{S_t}$. This seems to contradict [1] where a linear dependence was found. However, Equation 18 was derived with the assumption of an infinitely large layer thickness. Linear dependencies can be obtained for finite layer thicknesses [7, 8]. This will be verified in the following.

4.2. *Thin-film electrode*

If the maximum layer thickness of the cermet electrode, L, equals the penetration depth λ or is markedly smaller, Equation 12 with the formulation $e^x = 1 + x$ will be written as

$$i_d = \frac{1}{\rho_e} KL\eta(0) = S_t \frac{2F}{RT} L j_{00} \eta(0) \tag{24a}$$

that is, because of Equation 13 the following is true

$$j_0 = S_t L j_{00} \tag{24b}$$

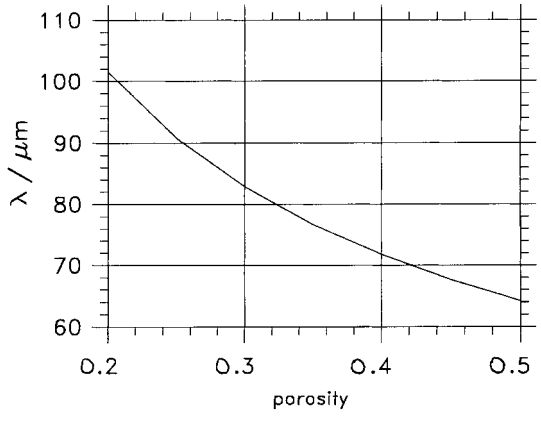

Fig. 5. Calculated dependence of the electrochemically active layer thickness λ on porosity for a constant pore diameter of 0.5 μm, working temperature 1223 K.

and a linear dependence between the measurable macrokinetic exchange current density j_0 and the active internal surface S_t is obtained. The same relation was also derived in [7] as the limiting case for active overvoltage regions with small overvoltages η and high macrokinetic current densities i_d.

The thin electrode solution is obtained through the introduction of the series $\exp[x] \cong 1 + x + x^2/2 + \cdots$ into Equation 12. Neglecting the third and higher order terms the fraction containing the exponentials becomes $x/(1 + x^2/2) \simeq x - x^2/2$, thus the relative error for $x = 1$ or $L/\lambda = 1$ is 50%.

5. Evaluation of the diffusion layer

The above approximate calculation for the thickness of the electrochemically active layer within the substrate anode is only justified if the concentration of hydrogen is kept constant at a reasonably specified current density within the penetration depth λ. For this reason, the electrochemically active layer thickness λ will be assigned a diffusion layer thickness δ_λ with the constant hydrogen concentration c, for which the condition of diffusion-controlled current is given according to the general equation

$$i_d = 2FD_{eff} \frac{(c_\delta - c_s)}{\delta_\lambda} \tag{25}$$

$D_{eff,\lambda}$ is the effective diffusion coefficient in the electrochemical layer, which depends on the porosity ε and the pore radius r_p and can be calculated according to the equation

$$\frac{1}{D_{eff,\lambda}} = \frac{1}{\varepsilon^2}\left(\frac{1}{D_g} + \frac{1}{D_{Kn}}\right) \tag{26}$$

D_g is the hydrogen diffusion coefficient of the free gas phase, which only depends on temperature. For the Knudsen diffusion coefficient D_{Kn} of hydrogen, the relation

$$D_{Kn} = 100 \frac{2}{3} r_p \sqrt{\frac{8RT}{0.002\,\pi}} \tag{27}$$

was derived [4]. It is then possible to estimate the homogeneity of distribution of the hydrogen concentration using the same input data as for the calculation of the electrochemical layer thickness. 'Constant' means that the hydrogen concentration changes by less than 5% at a typical current density of $i = 500\,\text{mA cm}^{-2}$ within the penetration depth λ. This diffusion layer thickness, δ_λ, is then calculated according to the formula

$$\delta_\lambda = \frac{2FD_{eff,\lambda} p_{H_2} \text{DIFF1}}{RTi_d} \tag{28}$$

where DIFF1 is the difference in concentration along the diffusion layer δ_λ relative to the entrance concentration p_{H_2}. DIFF1 has the value 0.05 in our case. The results of comparative calculations show that the diffusion layer δ_λ is always greater than the penetration depth of the electric field, that is, the assumptions for calculating the penetration depth are largely

Table 2. Dependence of the diffusion overvoltage on layer thickness for different D_{eff}, i_d = 500 mA cm^{-2}, $p^0_{H_2}$ = 0.6 bar, DIFF1 = 0.05, t = 950 °C, together with the corresponding values of DIFF2

D_{eff} /cm^2 s^{-1}	*1.00*	*1.10*	*1.20*	*1.30*	*1.40*	*1.50*	*1.60*
δ/μm				$-\eta$/mV			
1000	11.4	10.9	10.5	10.2	10.0	9.7	9.5
1200	12.3	11.8	11.4	11.0	10.7	10.4	10.1
1400	13.3	12.7	12.2	11.7	11.4	11.0	10.7
1600	14.2	13.5	13.0	12.5	12.0	11.7	11.4
1800	15.2	14.4	13.8	13.2	12.7	12.3	12.0
2000	16.1	15.3	14.6	13.9	13.4	13.0	12.6
2200	17.1	16.1	15.3	14.7	14.1	13.6	13.3
2400	18.1	17.0	16.1	15.4	14.8	14.2	13.8

D_{eff} /cm^2 s^{-1}	*1.00*	*1.10*	*1.20*	*1.30*	*1.40*	*1.50*	*1.60*
δ/μm				DIFF 2			
1000	0.041	0.038	0.034	0.032	0.030	0.028	0.026
1200	0.050	0.045	0.041	0.038	0.035	0.033	0.031
1400	0.058	0.053	0.048	0.045	0.041	0.039	0.036
1600	0.066	0.060	0.055	0.051	0.047	0.044	0.041
1800	0.074	0.068	0.062	0.057	0.053	0.050	0.046
2000	0.083	0.075	0.069	0.064	0.059	0.055	0.052
2200	0.091	0.083	0.076	0.070	0.065	0.061	0.057
2400	0.099	0.090	0.083	0.076	0.071	0.066	0.062

fulfilled. Consequently, the electrochemical properties of hydrogen oxidation are decisive for and limit the design of the electrochemically active layer. Mass transport plays no major role.

The remaining electrode layer of the SOFC substrate anode, δ, outside the electrochemically active fraction only serves for mass transport. Its operating function is to supply hydrogen to the electrochemically active λ layer, to rapidly remove the water vapour and to ensure a homogeneous low-loss distribution of the electric field. Since it has no particular electrochemical function and only acts as a current distributor, its conductivity is only determined by the electronic fraction σ_m which results from the following relation [4]:

$$\sigma_m = \frac{9.5 \times 10^5}{T} \exp\left(\frac{-1150}{T}\right) \tag{29}$$

This value means that practically no irregularities in the distribution of the potential field are visible any more with a layer thickness of about 1mm [4] and that only the diffusion is of interest. As was shown using the FIT computation [4], a largely homogeneous distribution of the gas concentration prevails in the layer. The diffusion overvoltage η_D is produced by the drop in concentration along the diffusion layer δ. Its value is given by the following equations:

$$\eta_D = \frac{RT}{2F} \ln\left[\frac{p^0_{H_2O} p^{\text{surface}}_{H_2}}{p^0_{H_2} p^{\text{surface}}_{H_2O}}\right] = \frac{RT}{2F} \ln\left[\frac{\left(1 - x^0_{H_2}\right)\text{DIFF}}{1 - x^0_{H_2}\text{DIFF}}\right] \tag{30}$$

DIFF = (1 − DIFF1) × (1 − DIFF2). The quantity DIFF2 has the same meaning for δ as DIFF1 for δ_λ. This relates to the hydrogen concentration $p^0_{H_2}$ which is equivalent to molar fraction $x^0_{H_2}$ in the inlet channels and is bound to the value of the effective diffusion coefficient $D_{\text{eff},\delta}$ by the relation

$$D_{\text{eff},\delta} = \frac{RT\delta i_d}{2F p^0_{H_2} \text{DIFF2}} \tag{31}$$

The following is true: δ = (electrode thickness) $-\min(\lambda, \delta_\lambda)$. The calculated dependence of the diffusion overvoltage η_D on the layer thickness δ as well as the corresponding values of DIFF2 are shown in Table 2. The values are in good agreement with those calculated using the FIT method [11].

References

[1] J. Divisek, Y. Volfkovich and R. Wilkenhöner, *J. Appl. Electrochem* **29** (1999) 153–163.
[2] J. S. Newman and C.W. Tobias, *J. Electrochem. Soc.* **109** (1962) 1183.
[3] J. Newman and W. Tiedeman, *AIChE J.* **21** (1975) 25.
[4] Ch. Bleise, J. Divisek, B. Steffen, U. König and J. W. Schultze, 'Model Calculation of the Planar SOFC by the Finite Volume Element Method', *Proceeding of the 3rd Symposium on Solid Oxide Fuel Cells* (edited by S. C. Singhal and H. Iwahara). The Electrochemical Society, Pennington, NJ, Vol. 93–4 (1993), p. 861–7.
[5] T. Weiland, *Particle Accelerators* **15** (1984) 245.
[6] H. P. Buchkremer, U. Diekmann, L. G. J. de Haart, H. Kabs, U. Stimming, D. Stöver, 'Advances in the anode supported planar SOFC technology' *Proceedings of the 5th International Symposium on Solid Oxide Fuel Cells* (edited by U. Stimming, S. C. Singhal, H. Tagawa and W. Lehnert), The Electrochemical Society, Pennington, NJ vol 97–40 (1997), p. 160–70.
[7] J. M. Bisang, K. Jüttner and G. Kreysa, *Electrochim. Acta* **39** (1994) 1297.
[8] A. Winsel, *Z. Elektrochemie* **66** (1962) 287.
[9] P. Holtappels, 'Die Elektrokatalyse an Nickel-Cermet Elektroden', PhD Dissertation, University of Bonn (1997).
[10] A. Ruder, H. P. Buchkremer, H. Jansen, W. Mallener, D. Stöver, *Surf. & Coating Technol.* **53** (1992) 71.
[11] W. Lehnert, Simulation von Hochtemperaturbrennstoffzellen, in 'Elektrochemische Verfahrenstechnik', (edited by U. Stimming and W. Lehnert (GDCh-Monographien Bd. 9, 1966), p. 197.